DESY 13-147
August 2013

Obtaining high degree of circular polarization at X-ray FELs via a reverse undulator taper

E.A. Schneidmiller and M.V. Yurkov

Deutsches Elektronen-Synchrotron (DESY), Notkestrasse 85, D-22607 Hamburg, Germany

Abstract

Baseline design of a typical X-ray FEL undulator assumes a planar configuration which results in a linear polarization of the FEL radiation. However, many experiments at X-ray FEL user facilities would profit from using a circularly polarized radiation. As a cheap upgrade one can consider an installation of a short helical (or cross-planar) afterburner, but then one should have an efficient method to suppress powerful linearly polarized background from the main undulator. In this paper we propose a new method for such a suppression: an application of the reverse taper in the main undulator. We discover that in a certain range of the taper strength, the density modulation (bunching) at saturation is practically the same as in the case of non-tapered undulator while the power of linearly polarized radiation is suppressed by orders of magnitude. Then strongly modulated electron beam radiates at full power in the afterburner. Considering SASE3 undulator of the European XFEL as a practical example, we demonstrate that soft X-ray radiation pulses with peak power in excess of 100 GW and an ultimately high degree of circular polarization can be produced. The proposed method is rather universal, i.e. it can be used at SASE FELs and seeded (self-seeded) FELs, with any wavelength of interest, in a wide range of electron beam parameters, and with any repetition rate. It can be used at different X-ray FEL facilities, in particular at LCLS after installation of the helical afterburner in the near future.

Preprint submitted to Phys. Rev. ST-AB

1 Introduction

Successful operation of X-ray free electron lasers (FELs) [1–3], based on self-amplified spontaneous emission (SASE) principle [4], opens up new horizons for photon science. One of the important requirements of FEL users in the near future will be polarization control of X-ray radiation. Baseline design of a typical X-ray FEL undulator assumes a planar configuration which results in a linear polarization of the FEL radiation. However, many experiments at X-ray FEL user facilities would profit from using a circularly polarized radiation. There are different ideas [5–13] for possible upgrades of the existing (or planned) planar undulator beamlines.

As a cheap upgrade one can consider an installation of a short helical afterburner. In particular, an electromagnetic helical afterburner will be installed behind the soft X-ray planar undulator SASE3 of the European XFEL. However, to obtain high degree of circular polarization one needs to suppress (or separate) powerful linearly polarized radiation from the main undulator. Different options for such a suppression (separation) are considered: using achromatic bend between planar undulator and helical afterburner [7,8]; tuning resonance frequency of the afterburner to the second harmonic of the planar undulator [9]; separating source positions and using slits for spatial filtering [13].

In this paper we propose a new method for suppression of the linearly polarized background from the main undulator: application of the reverse undulator taper. In particular, in the case of SASE3 undulator of the European XFEL, we demonstrate that soft X-ray radiation pulses with peak power in excess of 100 GW and an ultimately high degree of circular polarization can be produced. As for a comparison with the other methods, our suppression method is free, easy to implement, and the most universal: it can be used at SASE FELs and seeded (self-seeded) FELs, with any wavelength of interest, in a wide range of electron beam parameters, and with any repetition rate. It can be applied at different X-ray FEL facilities, in particular at LCLS after installation of the helical afterburner in the near future.

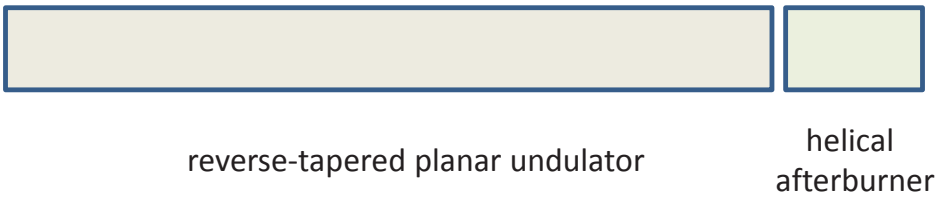

Fig. 1. Conceptual scheme for obtaining circular polarization at X-ray FELs.

2 Method description

In a short-wavelength SASE FEL the undulator tapering is used for two purposes: to compensate an electron beam energy loss in the undulator due to the wakefields and spontaneous undulator radiation; and to increase FEL power (post-saturation taper). In both cases the undulator parameter K decreases along the undulator length. The essence of our method is that we use the opposite way of tapering: parameter K increases what is usually called reverse (or negative) taper. We discover that in some range of the taper strength, the bunching factor at saturation is practically the same as in the reference case of the non-tapered undulator, the saturation length increases slightly while the saturation power is suppressed by orders of magnitude. Therefore, our scheme is conceptually very simple (see Fig. 1): in a tapered main (planar) undulator the saturation is achieved with a strong microbunching and a suppressed radiation power, then the modulated beam radiates at full power in a helical afterburner, tuned to the resonance.

Note that reverse undulator taper was considered in the past to increase saturation efficiency of FEL oscillators [15], and to produce attosecond pulses in X-ray FELs [16]. In this paper we discover a new useful feature of the reverse taper: a possibility to generate a strongly modulated electron beam at a pretty much reduced level of the radiation power.

To be specific, in this paper we will concentrate on the case of a helical afterburner and use the following formula for the degree of circular polarization:

$$D_{\rm cir} \simeq 1 - \frac{P_{\rm lin}}{2P_{\rm cir}} - F_{\rm A}, \tag{1}$$

where $P_{\rm lin}$ is the power of the linearly polarized radiation from the main undulator, $P_{\rm cir}$ is the power of the circularly polarized radiation from the helical afterburner. Factor of two in the denominator is easy to understand since the linearly polarized wave can be decomposed into left and right circularly polarized waves, and we consider the case when $P_{\rm lin} \ll P_{\rm cir}$. Except for a contamination due to linearly polarized background from the main undulator, a decrease of $D_{\rm cir}$ can be caused by field imperfections of the helical afterburner as well as by other sources of radiation of the modulated beam (edge radiation, coherent synchrotron radiation etc.) having different polarization properties. We describe all these possible contributions with a separate term $F_{\rm A}$. Note that even in the case of an ideal undulator, the term $F_{\rm A}$ can be of the order of inverse number of periods in the afterburner. Further discussions on this subject would go beyond the scope of this paper since our goal is to minimize the term $P_{\rm lin}/(2P_{\rm cir})$. We only notice here that there is not much sense to make it significantly smaller than the term $F_{\rm A}$. In most cases it means that a suppression of the term $P_{\rm lin}/(2P_{\rm cir})$ to a few per mil level is sufficient. Then we can state that a suppression scheme provides an ultimately high degree of circular polarization.

3 Selected results of the one-dimensional theory

A detailed theoretical analysis of the considered effect will be published elsewhere [17]. Here we present some selected results.

Let us consider the normalized detuning parameter [18]:

$$\hat{C} = \left(k_{\rm w} - \frac{\omega(1+K^2)}{2c\gamma^2} \right) \Gamma^{-1} \ . \tag{2}$$

The following notations are introduced here: $k_{\rm w} = 2\pi/\lambda_{\rm w}$ is the undulator wavenumber, ω is the frequency of the electromagnetic wave, K is the rms undulator parameter, γ is relativistic factor, and Γ is the gain parameter. The latter can be expressed in terms of the FEL parameter ρ [19]: $\Gamma = 4\pi\rho/\lambda_{\rm w}$.

We start our consideration with the case when a high-gain FEL is coherently seeded at a given frequency ω, and the undulator is not tapered. The properties of the FEL are then described by the detuning parameter (see, for example, [18] for more details). In

particular, in high gain linear regime (i.e. when the normalized undulator length $\hat{z} = \Gamma z \gg 1$) the squared modulus of the bunching factor $|b|^2$ and the normalized FEL power $\hat{\eta} = P/(\rho P_{\rm beam})$ are of the same order when an FEL operates close to the resonance, $|\hat{C}| < 1$. The normalized growth rate (inverse field gain length) of the FEL instability, $\mathrm{Re}\,\hat{\Lambda} = \mathrm{Re}\,\Lambda/\Gamma$, is of the order of unity in this regime. At the same time, the initial problem solution leads to an interesting result for a large negative detuning, $\hat{C} < 0$ and $|\hat{C}| \gg 1$. In this case the bunching factor and the normalized FEL power are connected in the high gain linear regime by a simple relation:

$$|b|^2 \simeq |\hat{C}|^2 \hat{\eta} \ , \tag{3}$$

i.e. the power is strongly suppressed with respect to the squared modulus of the bunching factor. Note that the tendency approximately holds at the FEL saturation. The normalized growth rate in the considered case gets smaller, $\mathrm{Re}\,\hat{\Lambda} \simeq |\hat{C}|^{-1/2}$, with the corresponding increase of the saturation length.

Now let us consider a SASE FEL with linearly tapered undulator. The normalized detuning parameter changes as follows:

$$\hat{C}(\hat{z}) = \beta \hat{z} \ , \tag{4}$$

where

$$\beta = -\frac{\lambda_{\rm w}}{4\pi\rho^2} \, \frac{K(0)}{1+K(0)^2} \, \frac{dK}{dz} \ , \tag{5}$$

and $K(0)$ is the initial value of the rms undulator parameter. Note that as a reference frequency we always consider the resonance frequency at the undulator entrance. Of course, in a SASE FEL a finite frequency band is amplified, and its maximum and width can evolve along the undulator length [20].

The theory of a high-gain FEL with varying undulator parameter has been developed in [20] in the limit of a small taper strength [1], $|\beta| \ll 1$. In particular, the authors of [20] have derived corrections to the FEL growth rate up to the second order. Unfortunately, we

[1] More strictly, the condition $|\beta|\hat{z} \ll 1$ is necessary.

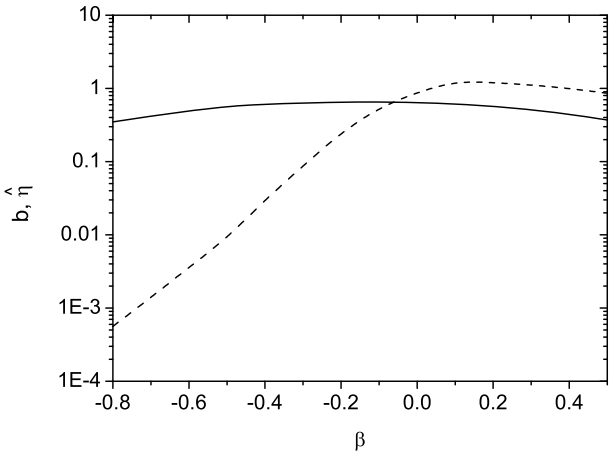

Fig. 2. Ensemble averaged rms bunching factor (solid) and normalized FEL efficiency (dash) at saturation point (position with maximum bunching factor) versus taper strength parameter. Energy spread parameter is $\hat{\Lambda}_{\rm T} = 0.2$.

cannot use the results of [20] for our purpose because, in the case of small corrections, the tendency we would like to demonstrate (small ratio $\hat{\eta}/|b|^2$) is not seen. For this reason we present here a result of the theory [17] that is valid in the case of a large taper strength. For a high-gain linear regime and a large negative taper strength, $\beta < 0$ and $1 \ll |\beta| \ll \hat{z}$, the relation between the ensemble-averaged squared modulus of the bunching factor $< |b|^2 >$ and the ensemble-averaged normalized FEL power $< \hat{\eta} >$ can be approximated as

$$< |b|^2 > \simeq |\beta|^2 \hat{z}^2 < \hat{\eta} > \ . \tag{6}$$

This equation looks similar to Eq. (3) with the detuning parameter given by (4). One can see that, indeed, for large negative β and large $\hat{z}$, the squared bunching factor is much larger than the normalized FEL power. Both quantities are proportional to $\exp(4\sqrt{\hat{z}/|\beta|})$, i.e. they evolve along the undulator length with a decreasing growth rate.

The asymptote of large negative β was considered here only for illustration of the power suppression effect. For practical applications we will restrict ourselves to moderate values of β which allow for a significant power suppression at strong bunching and an acceptable increase of the saturation length. We are interested in the values of bunching factor and FEL power at saturation, therefore we have to use a numerical simulation code (a linear analysis is not valid at saturation). Below we will use a simplified notation b instead of $\sqrt{< |b|^2 >}$. To make our results of 1-D simulation closer to practical cases, we

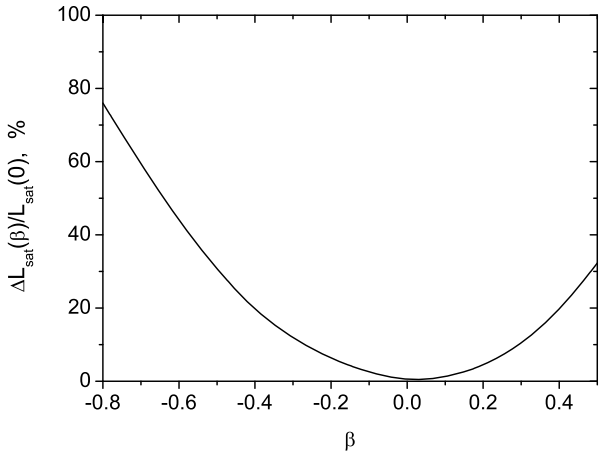

Fig. 3. Relative increase of the saturation length (defined as a length of the undulator at which maximum bunching is achieved) versus taper strength parameter. Energy spread parameter is $\hat{\Lambda}_{\rm T} = 0.2$.

also introduce an energy spread with a value typical for X-ray FELs. The energy spread parameter is defined as follows [18]: $\hat{\Lambda}_{\rm T} = \sigma_\gamma/(\gamma\rho)$ with σ_γ being the energy spread (in units of the rest energy). In our simulations we use the value $\hat{\Lambda}_{\rm T} = 0.2$. The results of simulations with 1-D version of the code FAST [21] are presented in Figs. 2 and 3.

In Fig. 2 we show the bunching factor and normalized FEL efficiency at saturation point which is defined here as the position where the maximum bunching is reached. One can see that for negative β the power quickly decreases (in contrast with positive β) although the bunching factor changes only slightly. From Fig. 3 one can find how the saturation length depends on the taper strength. A good range of this parameter for the proposed scheme is $\beta \simeq -0.5...-0.3$. Indeed, the bunching factor is still high in this range, there is only moderate increase of the saturation length, and the power is significantly suppressed.

4 Three-dimensional simulations for the European XFEL

The results of the previous Section were obtained in the framework of 1-D model. We found that the reverse taper method works well in 3-D case, and can even be more efficient than in 1-D case. We illustrate this with the parameters of the soft X-ray SASE3 undulator of the European XFEL [22]. Main parameters used in our simulations are presented in Table 1. The electron beam parameters are taken from the table provided by the European

XFEL beam dynamics group [23] for the bunch charge of 0.5 nC. We consider operation of SASE3 in "fresh bunch" mode [24] when the energy spread of electron bunches is not spoiled by the FEL interaction in the upstream SASE1 undulator. The simulations were performed with 3-D version of the code FAST [21].

A gap-tunable permanent-magnet SASE3 undulator consists of 21 undulator modules, each of them is 5 m long. One can easily control active part of the undulator by opening the gaps of the modules which are not needed. In our case we use only 11 last modules to adapt an active undulator length to the saturation length for the given wavelength (1.5 nm) and electron beam parameters. A long-period electromagnetic helical afterburner is being developed [25] for installation behind SASE3 undulator. The choice of technology is driven by the request of users to quickly change (between the macropulses, i.e. with the frequency of 5 Hz) the polarization of the output radiation between left and right.

We optimized the taper strength in the main undulator such that the radiation power is sufficiently suppressed, on the one hand, and the bunching factor is still close to that in the case of untapered undulator, on the other hand. We ended up with 2.1 % increase of K parameter over the undulator length of 55 m. According to (5), this corresponds to the one-dimensional [2] normalized taper strength of -0.34.

Evolution of the bunching factor along the planar undulator and the helical afterburner is shown in Fig. 4, and the time dependence of bunching factor at the exit of the planar undulator - in Fig. 5. One can see that the bunching factor reaches a pretty high level and becomes even larger in the helical afterburner.

Radiation power as a function of position in the planar main undulator and in the helical afterburner is shown in Fig. 6. One can see that, indeed, linearly polarized radiation from the main undulator is strongly suppressed (it is about 0.4 GW), and the powerful circularly polarized radiation quickly builds up in the afterburner. This happens because the bunching is strongly detuned from the resonance with the last part of the planar undulator, but the K value of the afterburner is optimized in such a way that it is close

[2] Note that in the considered case the one-dimensional normalization is not very convenient since the diffraction effects play a major role. If 1-D parameter ρ in (5) is substituted by the corresponding 3-D parameter [18], the taper strength is then -0.4.

Table 1
Main parameters used in simulations

Electron beam	
Energy	14 GeV
Charge	0.5 nC
Peak current	5 kA
Rms normalized slice emittance	0.7 μm
Rms slice energy spread	2.2 MeV
Planar undulator	
Period	6.8 cm
$K_{\rm rms}$	5.7
Beta-function	15 m
Active magnetic length	55 m
Taper $\Delta K_{\rm rms}/K_{\rm rms}(0)$	2.1 %
Helical afterburner	
Period	16 cm
K	3.6
Beta-function	15 m
Magnetic length	10 m
Radiation	
Wavelength	1.5 nm
Power from planar undulator, $P_{\rm lin}$	0.4 GW
Power from helical undulator, $P_{\rm cir}$	155 GW
$1 - P_{\rm lin}/(2P_{\rm cir})$	99.9 %

to the resonance, and maximum power is achieved at the end of the afterburner. A part of the radiation pulse is shown in Fig. 7 for illustration; ensemble averaged peak power reaches 155 GW. Now we can calculate the degree of circular polarization (not considering the term $F_{\rm A}$) due to contamination from the planar undulator: $1 - P_{\rm lin}/(2P_{\rm cir}) \simeq 0.999$. Note that a further suppression of the linearly polarized background and improvement of the quantity $1 - P_{\rm lin}/(2P_{\rm cir})$ is easily possible by going to a stronger taper at the price of

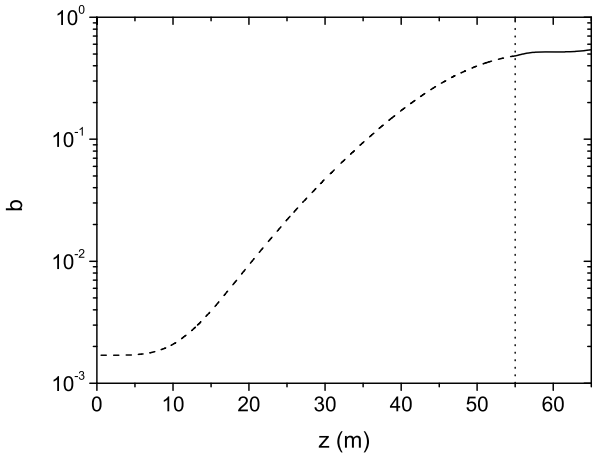

Fig. 4. Evolution of the ensemble averaged rms bunching factor along the planar undulator SASE3 (dash) and the helical afterburner (solid).

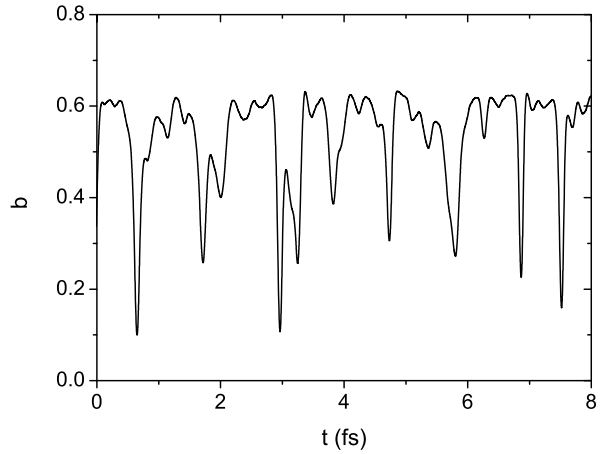

Fig. 5. Modulus of bunching factor versus time at the exit of the planar undulator SASE3 (position 55 m on Fig. 4). A central part of the electron bunch is shown.

a mild reduction of bunching factor (and, consequently, the power of circularly polarized radiation). However, this would probably make no sense because the degree of circular polarization would be mainly defined by the term $F_{\rm A}$, see the discussion above.

Parameters of the helically polarized radiation are shown in Table 1. The pulse duration and the pulse energy are defined by the chosen bunch charge (set of charges from 20 pC to 1 nC with different parameters will be available at the European XFEL). For example, the pulse duration can be chosen between few femtoseconds and 100 femtoseconds. In all cases the peak power and the degree of circular polarization will be comparable to

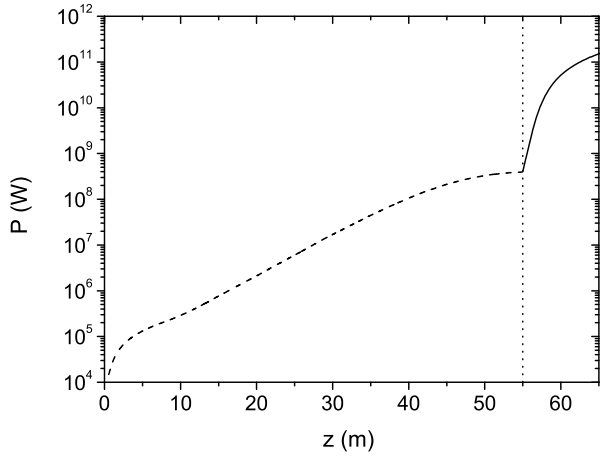

Fig. 6. FEL power versus the length of the planar main undulator SASE3 (dash) and the helical afterburner (solid).

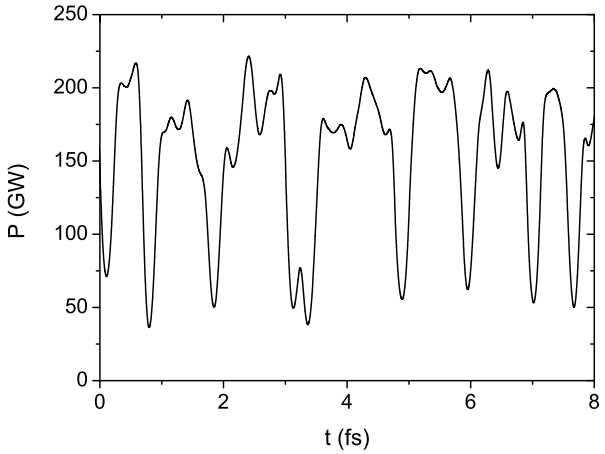

Fig. 7. Peak power of circularly polarized radiation at the exit of the afterburner (position 65 m on Fig. 6). A central part of the X-ray pulse is shown.

those shown in Table 1. Let us also notice that our method will work in a wide range of photon energies so that one can easily cover not only L-edges but also M-edges of all interesting elements. Indeed, in the considered case of lasing at 1.5 nm the active length of the undulator is 55 m (to be compared to the saturation length of 45 m for the untapered case, i.e. we have only 20% increase in length). The total magnetic length of the SASE3 undulator is 105 m so that there is a big reserve for going to shorter wavelength. Generally speaking, our method can also work at hard X-ray beamlines if this is requested by users.

Finally, let us note that in the case of energy loss along the undulator due to the wakefields

and spontaneous undulator radiation at high energies, the strength of the reverse taper can be decreased in accordance with formula (7), see discussion below. In our case both effects are small corrections, each of them is on the order of 0.1% in the active part of the SASE3 undulator - to be compared with about 2% of the K change.

5 A possible operation at LCLS

A fixed-gap planar undulator is used to generate hard- and soft- X-ray radiation at the Linac Coherent Light Source (LCLS) [2]. A helical afterburner is going to be installed soon in order to provide a circular polarization for user operation at LCLS [14].

Design of the planar undulator allows for a mild tapering by making use of canted poles. This option is normally used for compensation of the beam energy loss along the undulator length, and for the post-saturation taper - in both cases a standard (positive) sign of taper is needed. We propose here to use a reverse taper to obtain powerful X-ray radiation (in soft- and hard- X-ray regimes) with a high degree of circular polarization, in excess of 99%. Our estimates with the help of the formula (5) suggest that the strength of the reverse taper should typically be on the order of 1% over active undulator length. After optimizing the taper strength and active length of the main undulator, the K-value of the helical afterburner should be scanned in order to obtain maximum power. Such an experiment can be performed in the near future.

6 Some generalizations

For simplicity we have considered up to now the case when only the undulator parameter K changes linearly along the undulator length. Obviously, the parameter β can be generalized to the case when, in addition, the mean energy of electrons changes due to the wakefields and spontaneous undulator radiation:

$$\beta = -\frac{\lambda_{\rm w}}{4\pi\rho^2}\ \left[\frac{K(0)}{1+K(0)^2}\ \frac{dK}{dz} - \frac{1}{\gamma(0)}\frac{d\gamma}{dz}\right]\ . \tag{7}$$

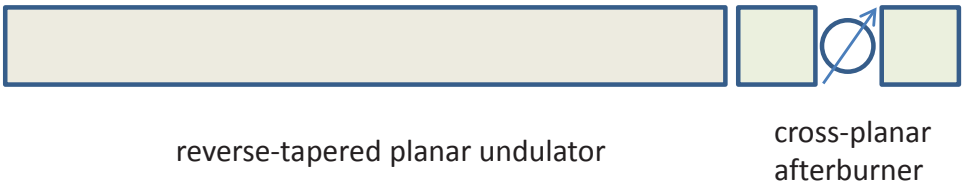

Fig. 8. Scheme for obtaining circular polarization in a cross-planar undulator.

Here $\gamma(0)$ is the gamma-factor at the undulator entrance. If the energy loss is not negligible, one should decrease the taper strength correspondingly.

We have mainly considered the case of a SASE FEL in this paper. In the case of seeded (self-seeded) FELs one can use two modifications of the suppression method: with reverse taper or with constant detuning of the K parameter (so that the detuning parameter $\hat{C}$ is negative).

We have simulated the helical afterburner for the SASE3 undulator of the European XFEL. Obviously, as an afterburner one can also consider a cross-planar undulator with a phase shifter [5,9] which may give more possibilities for polarization control. In this case the length of the afterburner should be short enough so that density modulation stays almost unchanged as the beam propagates in the afterburner. A more complicated cascaded crossed undulator [11,12] can be used as well.

7 Acknowledgements

We would like to thank R. Brinkmann, V. Balandin, N. Golubeva, W. Decking, and T. Limberg for useful discussions.

References

[1] W. Ackermann et al., Nature Photonics **1**(2007)336

[2] P. Emma et al., Nature Photonics **4**(2010)641

[3] T. Ishikawa et al., Nature Photonics **6**(2012)540544

[4] A.M. Kondratenko and E.L. Saldin, Part. Accelerators **10**(1980)207

[5] K.-J. Kim, Nucl. Instrum. and Methods **A 445**(2000)329.

[6] Y. Ding and Z. Huang, Phys. Rev. ST Accel. Beams 11(2008)030702.

[7] Y. Li et al., Proc. EPAC 2008 Conference, WEPC118, [http://www.jacow.org]

[8] Y. Li et al., Phys. Rev. ST-AB **13**(2010)080705

[9] E.A. Schneidmiller and M.V. Yurkov, Proc. of the FEL2010 Conference, Malmö, Sweden, p. 123, [http://www.jacow.org]

[10] E.A. Schneidmiller and M.V. Yurkov, Proc. of the FEL2010 Conference, Malmö, Sweden, p. 115, [http://www.jacow.org]

[11] T. Tanaka and H. Kitamura, AIP Conference Proceedings 705 (2004)231

[12] G. Geloni, V. Kocharyan and E. Saldin, preprint DESY-11-009, January 2011

[13] G. Geloni, V. Kocharyan and E. Saldin, preprint DESY-11-096, June 2011

[14] E. Allaria et al., Proc. of the FEL2011 Conference, Shanghai, China, August 2011, p. 31, [http://www.jacow.org]

[15] E.L. Saldin, E.A. Schneidmiller and M.V. Yurkov, Opt. Commun. **103**(1993)297

[16] E.L. Saldin, E.A. Schneidmiller and M.V. Yurkov, Phys. Rev. ST Accel. Beams **9**(2006)050702

[17] E.A. Schneidmiller and M.V. Yurkov, "Linear theory of a high-gain FEL with strongly tapered undulator", to be published

[18] E.L. Saldin, E.A. Schneidmiller and M.V. Yurkov, "The Physics of Free Electron Lasers", Springer, Berlin, 1999

[19] R. Bonifacio, C. Pellegrini and L.M. Narducci, Opt. Commun. **50**(1984)373

[20] Z. Huang and G. Stupakov, Phys. Rev. ST Accel. Beams **8**(2005)040702

[21] E.L. Saldin, E.A. Schneidmiller and M.V. Yurkov, Nucl. Instrum. and Methods **A 429**(1999)233

[22] M. Altarelli et al. (Eds.), XFEL: The European X-Ray Free-Electron Laser. Technical Design Report, Preprint DESY 2006-097, DESY, Hamburg, 2006 (see also http://xfel.desy.de).

[23] W. Decking, M. Dohlus, T. Limberg, and I. Zagorodnov, Baseline beam parameters for the European XFEL, private communication, December 2010

[24] R. Brinkmann, E.A. Schneidmiller and M.V. Yurkov, Nucl. Instrum. and Meth. **A 616**(2010)81

[25] N. Vinokurov et al., private communication